Manuscript

Title

Universal protection against SARS-CoV-2 viruses by multivalent mRNA vaccine in mice

Authors

Zhengyang Lei [a, b, †], Sumin Bian [c, †], Shiyao Zhai [a, b], Xi Yuan [a, b], Runming Wang [a, b], Pengyun Wang [a, b], Vijay Pandey [a, b], Can Yang Zhang [a, b], Dongmei Yu [b, d], Zhenglin Chen [a, b, *], Peiwu Qin [a, b, *]

[*]Email: pwqin@sz.tsinghua.edu.cn. Address: Lishui Road 2199, Nanshan District, Shenzhen, China 518055.

† This author contributed equally to this paper

Affiliations

[a] *Center of Precision Medicine and Healthcare, Tsinghua-Berkeley Shenzhen Institute, Shenzhen, Guangdong Province, 518055, China.*

[b] *Institute of Biopharmaceutics and Health Engineering, Tsinghua Shenzhen International Graduate School, Shenzhen, Guangdong Province, 518055, China.*

[c] *CenBRAIN, School of Engineering, Westlake University, Hangzhou, Zhejiang Province, 310030, China*

[d]*School of Mechanical, Electrical & Information Engineering, Shandong University, Weihai, Shandong province, 264209, China*.

Abstract

The ongoing emergence of new strains of Severe acute respiratory syndrome coronavirus 2 (SARS-CoV-2) variants challenges available SARS-CoV-2 vaccines for adequate control of outbreaks. Currently, there is a lack of universal vaccines for SARS-CoV-2 variants that do not necessitate strain matching between mRNA vaccines and the viruses. In this study, a nucleoside-modified twenty-valent lipid nanoparticle mRNA vaccine was designed and manufactured. The primary objective is to provide protection against various recent variants via the twenty-valent mRNA vaccine after efficacy assessment. Furthermore, the protection efficiency of bivalent and quadrivalent mRNA vaccines was compared with the universal vaccine. The neutralizing antibody activity against BA.4/5, XBB.1.5, BQ.1.1, and EG.5.1 was evaluated using enzyme-linked immunosorbent assay, pseudovirus neutralization test, and a rapid fiber-optic biolayer interferometry-based biosensor. Our universal multivalent vaccine provided robust protection against both prevailing and emerging, previously unidentified SARS-CoV-2 strains.

Introduction

The SARS-CoV-2 pandemic has caused 760 million infections and 6.9 million deaths (https://covid19.who.int). Over 13 billion vaccine doses have been administrated to prevent the virus transmission. However, the target antigens for most administrated vaccines are derived from

previously confirmed strains [1, 2]. The delay in vaccine development and the gradual emergence of mutant strains have led to a decrease in the efficacy of vaccination in providing protection against the most recent SARS-CoV-2 variants [3, 4].

SARS-CoV-2 invasion is primarily mediated by the binding between spike (S) protein and human angiotensin-converting enzyme-2 (hACE2). The S1 subunit of the S protein contains a receptor binding domain (RBD) responsible for the recognition and binding to the hACE2 [5, 6]. The S protein has been selected as a major target for vaccine development because of its important role in inducing host immune responses and neutralizing antibodies (NAbs) [7-9]. Omicron BA.1 was first identified in November 2021 and evolving strains including BA.2, BA.4, BA.5, BQ.1, XBB.1.5, and EG.5 were subsequently confirmed [10]. The accumulated mutation site in the spike protein of the Omicron variants facilitates evasion of antibody recognition [3, 11, 12]. To increase the vaccine protective efficiency, bivalent and quadrivalent vaccines were produced and evaluated [13-16]. The bivalent vaccine conferred protection in mice against previously circulating SARS-CoV-2 including BA.1 and BA.4/5 strains [13]. The quadrivalent vaccine was confirmed for its protection against B.1.351 variant [16]. The RBD trimer mRNA vaccine was able to protect against B.1.351 and B.1.617.2 variants [17]. Nevertheless, the protection efficacy of these vaccines against the latest strains such as XBB.1.5 and EG.5.1 has not yet been evaluated due to the rapid evolution of SARS-CoV-2[18]. Moreover, CH.1.1 and CA.3.1, two Omicron variants identified before EG.5.1, exhibit nearly complete escape of neutralization from bivalent booster [19]. Although deep learning and machine learning have been applied to predicting the antigenic evolution of SARS-CoV-2, an effective universal SARS-CoV-2 vaccine providing protection against the newest strains is urgently needed, and the protection efficiency of the vaccines on the market should be reassessed against new virus variants [20-23].

Multivalent vaccines have been developed to protect against the Influenza Virus and Human Papillomavirus. which successfully elicited high levels of cross-reactive and subtype-specific antibodies [1, 24]. Increasing evidence suggests that a multivalent SARS-CoV-2 vaccine may overcome the loss in efficacy of the current vaccine against persistent emerging Omicron variants. Furthermore, the mRNA vaccine has exhibited considerable efficacy, safety, and cost-effectiveness in its manufacturing process [25, 26]. Additionally, various of materials have been developed for delivering mRNA, including polymers, lipids, and protein derivatives. Especially, lipid nanoparticles (LNP) have been extensively investigated and have demonstrated successful clinical application in delivering mRNA [27-29]. Moderna LNP formulation was adopted in this study due to its superior efficacy in intramuscular delivery of mRNA and antibody production [30-32]. Therefore, a novel multivalent LNP-mRNA SARS-CoV-2 vaccine was designed and manufactured, followed by careful evaluation of its protection efficacy in mice.

In this study, we designed a nucleoside-modified multivalent mRNA vaccine. Hexaproline and two alanine substitutions were introduced into each variant of concerns (VOCs) and variantI of interests (VOIs) [33, 34]. Twenty valent vaccine covered the strains VOCs and VOIs including wuhan-1, B.1.1.7, B.1.351, P.1, B.1.525, B.1.526, B.1.617.1, B.1.427, B.1.429, B.1.617.2, AY.1, B.1.1.529, BA.1, BA.1.1, BA.2.7.5, BA.2.12.1, BA.4.6, BA.4/5, XBB.1, and XBB.1.5. After the characterization of the physicochemical properties of the produced LNP-mRNA, mRNAs were in vitro-transcribed and quantified to create a cocktail of mRNA mix with equal molar concentration for

individual mRNA specie. After the characterization of the physicochemical properties of the produced LNP-mRNA, mRNAs are confirmed to be encapsulated in the LNP particle with high packing efficiency. BALB/c mice were used as experimental animals to evaluate the protein efficacy of universal vaccine. We evaluated in mice the antibody responses against the prevailing Omicron variants including BA.4/5, BQ.1.1, XBB.1.5, and EG.5.1. Besides, the protection efficacy of mRNA vaccines including mRNA-1273 (Wuhan-1), mRNA-1273.214 (Wuhan-1/BA.1), mRNA-XBB.1.5, and mRNA-quadrivalent (Alpha/Beta/Delta/BA.1) were investigated as control. The activity of NAbs was evaluated in the serum of mice immunized with the vaccines using multiple methods including the standard enzyme-linked immunosorbent assay (ELISA), pseudovirus neutralization test, and a rapid fiber-optic biolayer interferometry-based (FO-BLI) biosensor, which minimize the assessment bias of single assay [35]. The results demonstrated that monovalent, bivalent, and quadrivalent vaccines cannot provided protection against new XBB.1.5 and BQ.1.1 strains, where BQ.1.1 strain is not included in our universal vaccine design. Meanwhile, the proposed multivalent vaccine can provide universal protection against previously and currently circulating SARS-CoV-2 variants. Our results provided the basis for the advancement of next-generation universal vaccine against SARS-CoV-2 variants.

Results

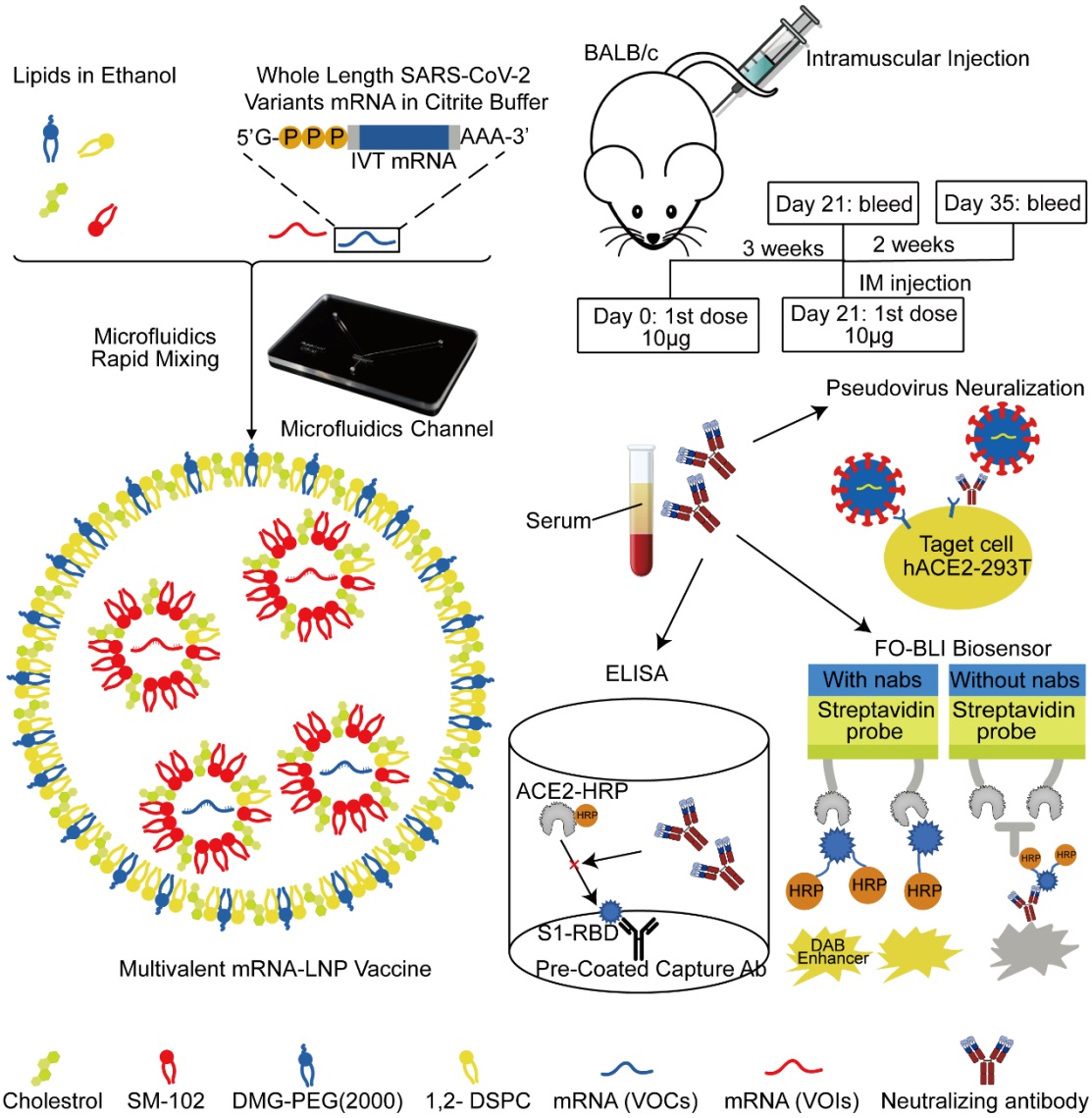

Figure 1. Schematic of the multivalent mRNA vaccine production and its protection efficacy evaluation. 5'-cap mRNAs of VOCs and VOIs were obtained by in vitro transcription and two-step enzymatic reactions. Four lipids dissolved in ethanol and mRNA dissolved in citrate buffer were rapidly mixed using microfluidics to formulate mRNA-LNP. mRNA-LNP vaccine is administrated to BALB/C mice via intramuscular injection. Serum samples from immunized mice were collected after the first and second boost immunization. The NAbs activity against the latest SARS-CoV-2 variants was evaluated by ELISA, pseudovirus neutralization, and FO-BLI biosensor. DAB: 3,3′-diaminobenzidine tetrahydrochloride. VOCs: variants of concerns, VOIs: variants of interests. IVT: in vitro transcription.

The administration of bivalent and quadrivalent vaccines that include targeting antigens such as the Omicron, Alpha, Beta, Gamma spike, and the Wuhan-1 spike could broaden immunity against variants of SARS-CoV-2. We proposed multivalent mRNA vaccine protection efficacy with the aim of dramatically increasing the protection spectrum of SARS-CoV-2 variant. We prepared a total of five lipid nanoparticles (LNP)-encapsulated mRNA vaccines including mRNA-1273, mRNA-1273.214, mRNA-XBB.1.5, mRNA-quadrivalent, and mRNA-multivalent to compare their relative

efficacy where mRNA-1273, mRNA-1273.214, mRNA-XBB.1.5, mRNA-quadrivalent are clinically used. The mRNA constructs design including 5' untranslated region (5'-UTR), protein coding sequence (CDS), and 3'-UTR was summarized **(Figure 2A)**. The 5'-UTR derived from human α-globin gene was used due to its superior translation efficiency [36]. Hexa-proline and alanine substitutions were introduced to the spike coding sequence of each SARS-CoV-2 strain. The 3'-UTR was a combination of the amino-terminal enhancer (AES) and the human mitochondrial 12S rRNA (mtRNR1), which contributed to increasing protein expression and mRNA stability [37]. These sequences were followed by a 30-mer poly (A) tail, a 10-nucleotide linker sequence (GCAUAUGACU), and 70 adenosine residues, which enhanced protein expression and could be in vitro transcribed from the DNA template without poly (A) addition [38]. Besides, the optimization of the CDS region was consistent with sequence derived from moderna-1273. Furthermore, Hexa-proline and two alanine substitutions were introduced to wuhan-1, VOCs and VOIs mRNA structure. The LNP formulation and production of LNP-mRNA vaccine was adopted as previously described **(Figure 2B)** [17]. Gel electrophoresis was used to evaluate mRNA integrity **(Figure 2C)**. Physiochemical characterization of each mRNA-LNP vaccine was conducted **(Figure 2D and S1A)**. The uniform size distribution was corroborated by a transmission electron microscope (TEM) **(Figure S1B)**.

A

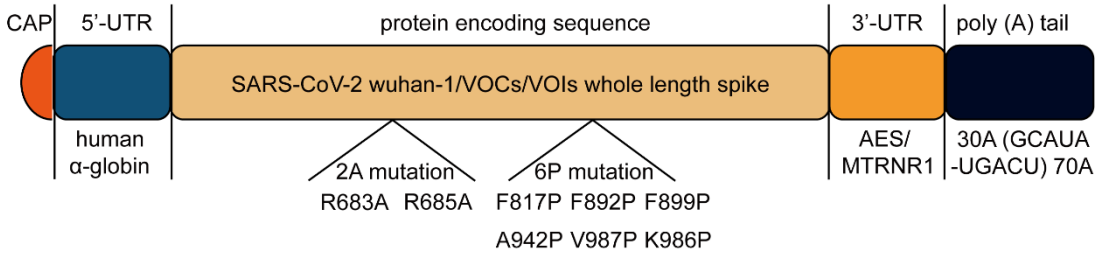

B

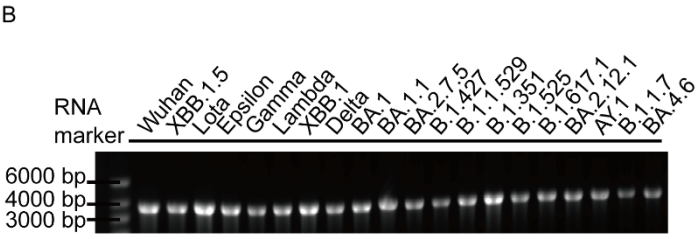

C

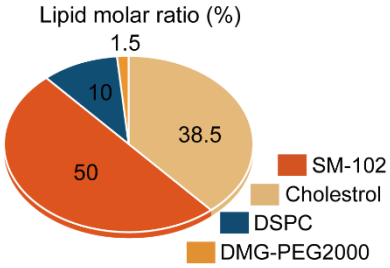

D

	Size (nm)	PDI	Zeta potential (mv)	Encapsulation rate (%)
mRNA-1273	103.4 ± 0.8083	0.177 ± 0.031	-1.01 ± 0.586	89.51
mRNA-XBB.1.5	95.45 ± 3.323	0.168 ± 0.020	-1.26 ± 0.485	90.41
mRNA-1273.214	97.59 ± 1.672	0.162± 0.019	-1.08 ± 0.350	92.99
mRNA-quad	89.83 ± 1.852	0.140 ± 0.031	-1.30 ± 0.238	88.8
mRNA-multi	88.44 ± 1.478	0.173 ± 0.015	-0.882 ± 0.387	89.97

Figure 2. Physicochemical characterization of mRNA-LNPs. (A) Schematic representation of mRNA constructs. (B) Agarose gel electrophoresis of in vitro transcribed mRNA products. (C) A pie chart showing the molar ratio of lipids for LNP formulation. DSPC: 1,2-Distearoyl-sn-glycero-3 phosphocholine, DMG-PEG2000: 1-monomethoxypolyethyleneglycol-2,3-dimyristylglycerol with

polyethylene glycol of average molecular weight 2000. (D) Table summarizing mRNA-LNP vaccine physiochemical parameters.

As described in **Figure 3A**, we first immunized BALB/c mice twice at a 3-week interval with 10 μg (total dose) of each vaccine. Three weeks after the first dose (on day 21) and 2 weeks after the second dose (on day 35), we tested the inhibitory capabilities of serum antibodies against XBB.1.5 strain. These antibodies were obtained from BALB/c mice who had received two doses of the mRNA-multivalent vaccine, in addition to another mRNA vaccine. ELISA results on day 21 showed that inhibitory activity of NAbs was highest in sera of mice vaccinated with mRNA-XBB.1.5, followed by mRNA-multivalent. The remaining groups, including those vaccinated with mRNA-1273, mRNA-1273.214, and mRNA-quadrivalent did not exhibit robust neutralizing antibody responses. Besides, ELISA results on day 35 demonstrated that a booster dose of vaccine resulted in a heightened level of neutralizing antibody activity **(Figure 3B).** Next, we evaluated their protection efficacy against other previously prevailing SARS-CoV-2 strains including BA.4/5 and BQ.1.1. Results further indicated that the mRNA-multivalent and mRNA-XBB.1.5 exhibited enhanced efficacy in inhibiting these two strains **(Figure 3C)**. A vesicular stomatitis virus (VSV)-based neutralization assay, with pseudoviruses displaying spike proteins of the latest prevailing XBB.1.5, BQ.1.1, and BG.5.1, was conducted to confirm the findings **(Figure S2)**. Low levels of neutralizing antibody against XBB.1.5 were induced by mRNA-1273 (GMT: 92), mRNA-1273.214 (GMT:115), and mRNA-quadrivalent (GMT: 108). The mRNA-XBB.1.5 (GMT: 3470) and mRNA-multivalent (GMT: 2233) showed a strong inhibitory response against XBB.1.5 **(Figure 3D)**. Besides, the mRNA-multivalent showed a strong inhibitory response against BQ.1.1 (GMT: 5134) but induced lower levels of neutralizing antibody against EG.5.1 (GMT: 1563). Mice vaccinated with mRNA-XBB.1.5 showed greater neutralizing antibody response against EG.5.1 (GMT: 4195) and lower neutralizing activity against BQ.1.1 (GMT: 763).

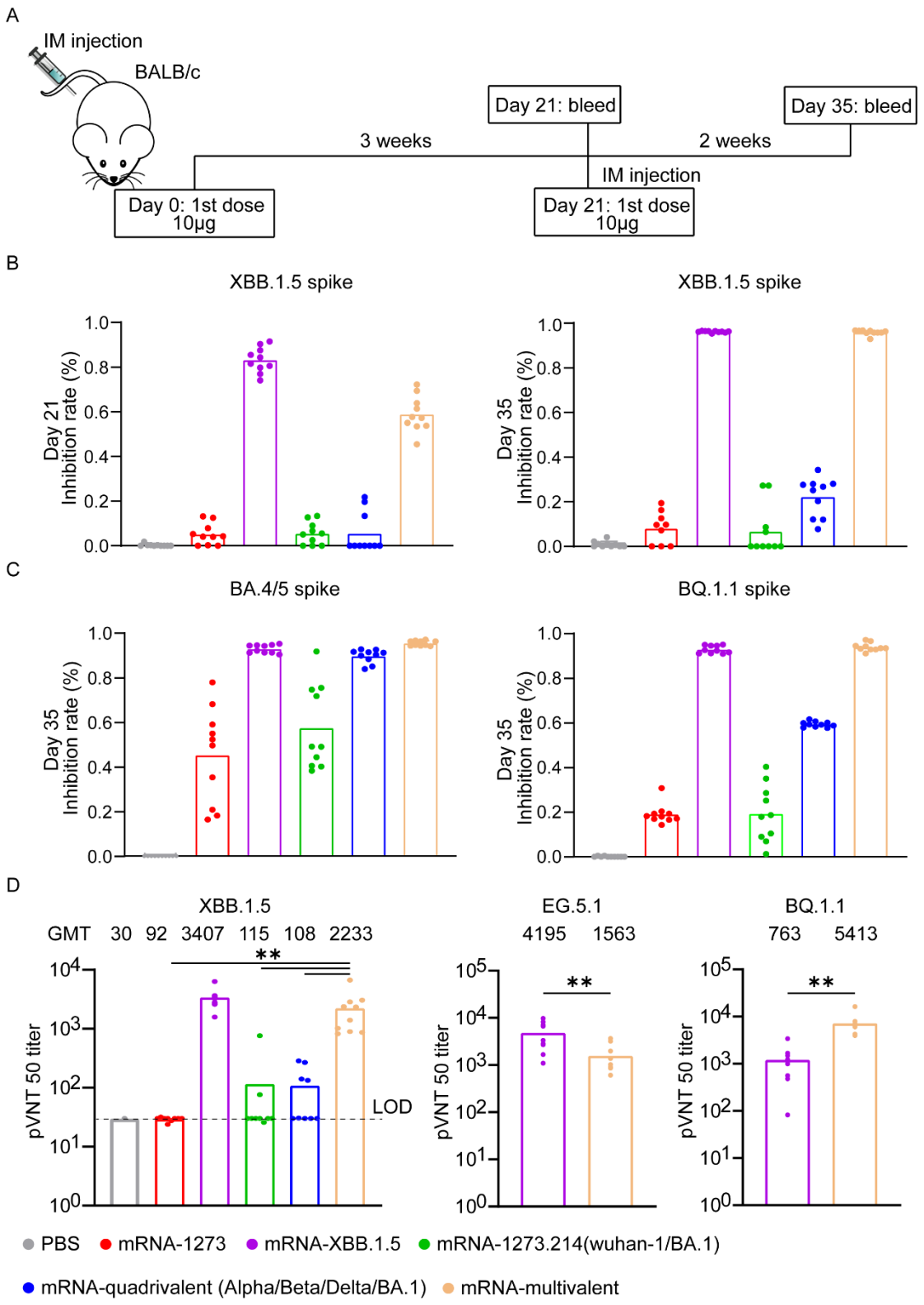

Figure 3. Neutralizing antibody responses in BALB/c mice after immunization with multivalent vaccine and state-of-the-art vaccines. (A) Six-to-eight-week-old BALB/c mice were immunized over a 3-week interval with PBS or 10 μg dose of mRNA vaccine in total. Mice serum was collected at 3 weeks following the initial vaccine administration and 2 weeks following the second boost vaccination. (B) Serum neutralizing antibody activity against XBB.1.5 evaluated by

ELISA at day 21 and day 35 (n = 10 mice per group in per experiment). (C) Serum neutralizing antibody activity against BA.4/5 and BQ.1.1 evaluated by ELISA at day 35. (D) Neutralizing activity of serum at day 35 against VSV pseudoviruses displaying the spike proteins of XBB.1.5, EG.5.1, or BQ.1.1 n=10 per mice group, one experiment; tops of boxes show the geometric mean of neutralizing antibody titer (GMT), which are indicated above each column, and dotted lines show limit of detection (LOD).

To further validate our results, we used FO-BLI biosensors to detect the specific NAbs in vaccinated mise serum. The principle of FO-BLI was as described **(Figure 4A)**. mRNA-XBB.1.5 and mRNA-multivalent induce strong specific NAbs against BA.4/5 and BQ.1.1, which was consistent with the results obtained from ELISA and VSV-based pseudovirus neutralization tests **(Figure 4B)**. Next, the serum samples from mice with vaccinated mRNA-multivalent and mRNA-XBB.1.5 were mixed to evaluate the inhibitory activity of the NAbs. The results showed that mRNA-multivalent and mRNA-XBB.1.5 provides strong vaccination efficacy **(Figure 4C)**.

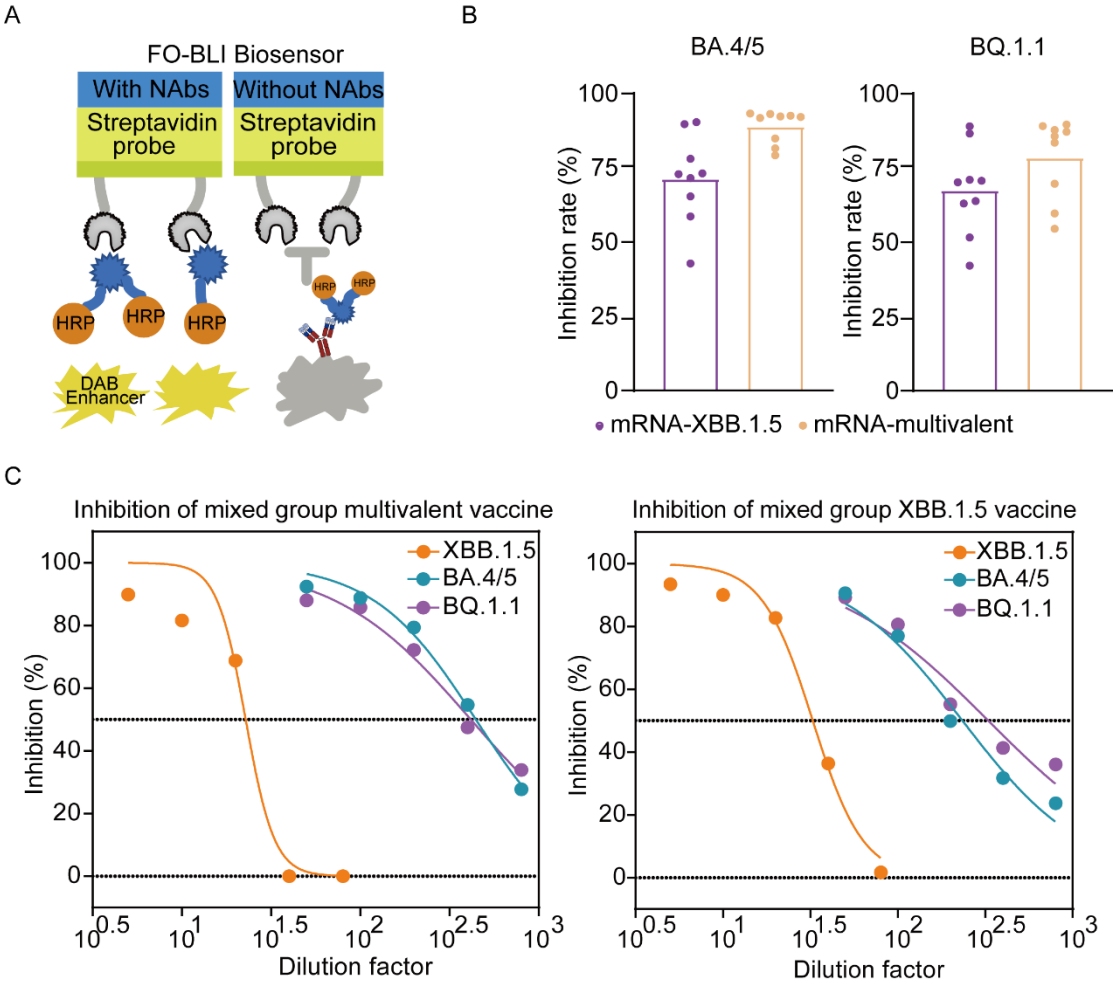

Figure 4. Neutralizing antibody activity evaluated by FO-BLI biosensor. (A) Principle of the FO-BLI biosensor for detection of NAbs via a competitive binding format. In the absence of NAbs, the interaction between the HPR-RBD domain of the SARS-CoV-2 spike protein and hACE2 leads to strong detection signals. Conversely, the presence of NAbs inhibits the binding of HRP-RBD to immobilized hACE2 protein. The optical signals were significantly enhanced by the addition of DAB in both bioassays. (B) Serum neutralizing antibody activity against BA.4/5 and BQ.1.1 evaluated by FO-BLI biosensor at 35 (n= 9 mice per group, one experiment). (C) Grouped serum neutralizing

antibody activity against BA.4/5, BQ.1.1, and XBB.1.5. The serum from each mouse, which had been injected with multivalent or XBB.1.5 vaccine, was mixed into a single sample and assayed for neutralizing antibody activity (n= 9 mice per sample).

Discussion

To evaluate the protection efficacy of the proposed universal mRNA vaccine, multiple methods were utilized to detect the NAbs activity. The results from the three methods showed a high level of consistency. Variant-specific candidate vaccines, mRNA-XBB.1.5 and mRNA-multivalent, induced robust serum antibody responses that effectively neutralized XBB.1.5 variant **(Figure 3B and 3D)**. On the other hand, the mRNA-1273, mRNA-1273.214, and mRNA-quadrivalent vaccines failed to induce specific Nabs against XBB.1.5 variant **(Figure 3B)**. However, mRNA-1273.214 and mRNA-quadrivalent continued to exhibit effectiveness in protecting against previously circulating variants, such as BA.4/5 and BQ.1.1 **(Figure 3C)**. Our findings indicated that both variant-specific and multivalent vaccines provided superior protection against the recent XBB.1.5 variant. The discovery carries significant implications for vaccine administration, serving as a valuable reference for both commercial production and clinical application.

The emergence of EG.5.1 variant occurred after the initiation of this study, and as a result, no variant-specific vaccine targeting EG.5.1 was developed. Nonetheless, both the mRNA-XBB.1.5 and mRNA-multivalent demonstrated remarkable protection efficacy against EG.5.1 variant **(Figure 3D)**. This aligns with the latest findings from Moderna [39]. In contrast to the recurrent seasonal influenza viruses, the mutation and evolution of SARS-CoV-2 tends to be more unpredictable [40, 41]. While rapid and large-scale SARS-CoV-2 genome sequencing can aid in monitoring its evolution, it necessitates enormous resources in terms of materials and finances [42, 43]. The mRNA-multivalent vaccine holds great promise in protecting against potential mutated variant since it induces cross-reactive and subtype specific-antibodies. Besides, the mRNA-multivalent elicited neutralizing activity against several currently circulating variants **(Figure 4B and 4C)**. Therefore, this proposed universal mRNA-multivalent is poised to play a pivotal role in preventing the COVID-19 pandemic.

Conclusion

In this study, we introduced an innovative twenty-valent SARS-CoV-2 mRNA vaccine. Our findings conclusively reveal that the mRNA-multivalent vaccine elicited potent, universal neutralizing activity against a spectrum of variants, including BA.4/5, BQ.1.1, XBB.1.5, and EG.5.1 variants. We firmly believe this novel mRNA-multivalent vaccine can establish a valuable foundation and provide critical insight for the development of a universal SAR-CoV-2 vaccine.

Materials and Methods

Mice

BALB/c mice aged 6-8 weeks were purchased from Bestest Biotechnology Co., Ltd and subsequently housed at TOP Biotechnology Co., Ltd. Animal experiments were carried out in compliance with approval from the Animal Care and Use Committee of the TOP Biotechnology Co.,

Ltd.

Construction of expression vectors encoding the wuhan-1, VOCs and VOIs spike of SARS-CoV-2

Condon-optimized full-length SARS-CoV-2 wuhan-1, VOCs, and VOIs spike were constructed and verified by sequencing, then cloned into a pSLQ1651-sgTelomere (F+E) vector. Proline substitutions (F817P, A892P, A899P, A942P, K986P, and V987P) and alanine substitutions (R683A and R685A) were introduced to each expressing vector to stabilize the trimeric prefusion state of SARS-CoV-2 S protein and enhance immunogenicity. Besides, spike genes contained the following mutations: (a) B.1.1.7: N503Y, A572D, D616G, P683H, T718I, S984A, D1120H, Δ69-70, and Δ144; (b) 1.3.5.1: L18F, D80A, D217G, R248I, K419N, E486K, N503Y, D616G, and A703V; (c) P.1: L18F, T20N, P26S, D138Y, R190S, K419T, E486K, N503Y, D616G, H657Y, T1029I, and V1178F; (d) B.1.525: Q52R, A67V, E486K, D616G, Q679H, F890L, Δ69-70, and Δ144; (e) B.1.526: L5F, T95I, D255G, E486K, D616G, A703V, and F890P; (f) B.1.617.1: T95I, G142D, E154K, L454R, E486Q, D616G, P683R, and Q1073H; (g) B.1.427: L454R, and D616G; (h) B.1.429: C131I, W152C, L454R, and D616G; (i) B.1.617.2 : T19R, G142D, E156G, L454R, T480K, D616G, P683R, D952N, and Δ157-158; (j) AY.1: T19R, V70F, A224V, W260L, K419N, L454R, T480K, D616G, P683R, D952N, and Δ157-158; (k): B.1.1.529: A67V, T95I, G142D, N211I, L212V, V213R, Δ214E, Δ215P, R216E, G341D, S373L, S375P, S377F, K419N, N442K, G448S, S479N, T480K, E486A, Q495R, G498S, Q500R, N503Y, Y507H, T549K, D616G, H657Y, N681K, P683H, N766K, D798Y, N858K, Q956H, N971K, L983F, Δ69-70, and Δ143-145; (l) BA.2.12.1: T19I, A27S, G142D, V213G, G341D, S373F, S375P, S377F, T378A, D407N, R410S, K419N, N442K, L454Q, S479N, T480K, E486A, Q495R, Q500R, N503Y, Y507H, D616G, H657Y, N681K, P683H, A685G, A687G, S706L, N766K, D798Y, Q954H, N971K, and Δ24-26; (m) BA.1.1: A67V, T95I, G142D, N211I, L212V, V213R, Δ214E, Δ215P, R216E, G341D, R348K, S373L, S375P, S377F, K419N, N442K, G448S, S479N, T480K, E486A, Q495R, G498S, Q500R, N503Y, Y507H, T549K, D616G, H657Y, N681K, P683H, N766K, D798Y, N858K, Q956H, N971K, L983F, Δ69-70, and Δ143-145; (n) BA.2.7.5 : T19I, A27S, G142D, K147E, W152R, F157L, I210V, V213G, G259S, G341H, S373F, S375P, S377F, T378A, D407N, R410S, K419N, N442K, G448S, N462K, S479N, T480K, E486A, Q500R, N503Y, Y507H, D616G, H657Y, N681K, P683H, N766K, D798Y, Q956H, N971K, and Δ24-26; (o) BA.4.6: T19I, A27S, G142D, V213G, G341D, R348T, S373F, S375P, S377F, T378A, D407N, R410S, K419N, N442K, L454R, S479N, T480K, E486A, F488V, Q500R, N503Y, Y507H, D616G, H657Y, N660S, N681K, P683H, N766K, D798Y, Q956H, N971K, Δ24-26, and Δ69-70; (p) BA.1: A67V, T95I, G142D, N211I, L212V, V213R, Δ214E, Δ215P, R216E, G341D, S373L, S375P, S377F, K419N, N442K, G448S, S479N, T480K, E486A, Q495R, G498S, Q500R, N503Y, Y507H, T549K, D616G, H657Y, N681K, P683H, N766K, D798Y, N858K, Q956H, N971K, L983F, Δ69-70, Δ143-145, and Δ1276, (q) BA.4/5: T19I, A27S, G142D, V213G, G341D, S373F, S375P, S377F, T378A, D407N, R410S, K419N, N442K, L454R, S479N, T480K, E486A, F488V, Q500R, N503Y, Y507H, D616G, H657Y, N681K, P683H, N766K, D798Y, Q956H, N971K, Δ24-26, and Δ69-70; (r) ΔBB.1: T19I, A27S, V83A, G142D, H146Q, Q183E, V213E, G341H, R348T, L370I, S373F, S375P, S377F, T378A, D407N, R410S, K419N, N442K, V447P, G448S, N462K, S479N, T480K, E486A, F488S, F492S, Q500R, N503Y, Y507H, D616G, H657Y, N681K, P683H, N766K, D798Y, Q956H, N971K, Δ24-26, and Δ144; (s) ΔBB.1.5: T19I, A27S, V83A, G142D, H146Q, Q183E, V213E, G341H, R348T, L370I, S373F, S375P, S377F, T378A, D407N, R410S, K419N, N442K, V447P, G448S, N462K, S479N, T480K, E486A, F488S, F492S,

Q500R, N503Y, Y507H, D616G, H657Y, N681K, P683H, N766K, D798Y, Q956H, N971K, Δ24-26, and Δ144.

Design and production of lipid-nanoparticle encapsulated mRNA vaccines

The mRNA was transcribed from the linearized DNA templated using T7 RNA polymerase reaction with complete replacement of uridine by N1m-pseudouridine (Vazyme, DD4202). The transcription products were then purified (New England Biolabs, T2050L) and the cap1 tructure was added for efficient translation and evading the cellular innate immune response (New England Biolabs, M2081 and M0366). Lipid-nanoparticle (LNP) formulation of mRNA was performed as previously described. Briefly, lipids were dissolved in absolute ethanol containing an ionizable lipid SM-102, 1, 2-distearoly-sn-glycero-3-phosphocholine (DSPC), cholesterol, and PEG-lipid with a total molar weight 8 mM and the molar ratio of 50:10:38.5:1.5. The lipid mixture was combined with 50 mM citrate buffer (pH 4.0) containing mRNA at an N/P ratio of 6:1, a flow rate ratio of 3:1, and total flow rate 12 ml/min through a T-mixer. Formulations were then diafiltrated against 30× volumes of PBS (pH 7.4) through a tangential-flow filtration (TFF) membrane with 30 KD molecular weight cut-offs. 10% sucrose was added as a cryoprotectant. The final solution was sterile-filtered passing through a 0.22 μm filter and stored at -20 ℃ for further use. All formulations were tested for particle size, distribution, RNA concentration and encapsulation.

Quality control of LNP-mRNA

Encapsulation of mRNA in the LNP was measured using a Quani-it™ RiboGreen™ RNA Assay Kit according to the manufacturer's instructions (ThermoFisher Scientific, R11491). The size, polydispersity (PDI) and zeta-potential of mRNA-LNP were measured by dynamic light scattering (DLS) on a Zeta sizer Nano ZS (Malvern instruments, UK). LNP-mRNA was diluted 100 times in PBS (pH 7.4) and added to a cuvette. The dispersant (PBS) refractive index (RI), viscosity values, and material RI were 1335, 1.02, and 1.45, respectively. Scattered light was detected at a backscattering angle of 173°. Results were analyzed using software of Zeta sizer V7.13. The morphology of LNP-mRNA was investigated using the FEI Tecnai T12 G2 cryo-TEM. The samples were stained with 2% uranylacetate as previously described [16].

SARS-CoV-2 Surrogate Virus Neutralization Test (sVNT) kit (ELISA)

To detect the amount and inhibition rate of neutralizing antibodies from the serum of immunized mice against VOCs, the commercialized ELISA kit (Genscript, Cat#L00871) was used. The tests were conducted according to the manufacture's protocol. Briefly, the kit and serum samples were removed and left at room temperature (20-25 ℃) before running the assay at least 30 min. Serum samples were diluted with sample dilution buffer with a volume ratio of 1:9. Standard stocks were serially diluted as described in the protocol to establish the standard calitration curves. Probe RBD (XBB.1.5, BQ.1.1, and BA.4/5) and enzyme conjugate were diluted with assay buffer with a volume ratio of 1:2000. The diluted serum samples and probe RBD working solution were mixed in a volume

ratio of 2:1 and incubated at 37 ℃ for 30 min. 100 μL mixture was transferred to the captured plate, which was then covered by a plate sealer and incubated at 30 ℃ for 15 min. Then, the plate was washed with 1× wash solution four times. The residual liquids in the wells were totally removed and 100 μL enzyme conjugate working solution was added. The sealed plate was incubated at 37 ℃ for 15 min and repeat the wash steps. 100 μL TMB solution was added and the plate was incubated in the dark at 20-25℃ for 15 min. 50 μL Stop solution was added to each well. Finally, the absorbance at 450 nm was recorded immediately (Spark Tecan, Switzerland).

VSV Pseudovirus neutralization assay

hACE2-HEK293T cells were used as target cells for the neutralization assay and maintained in DMEM supplemented with 10% FBS. To perform the neutralization assay, immunized mice serum samples were heat-inactivated for 45 minutes at 56 ℃. The sera at a starting dilution of 1:30 (six dilutions) were threefold diluted with DMEM, and then mixed with an equal volume of pre-titrated pseudotyped virus. After incubation at 37 ℃ for 2 h, the inoculum or virus-serum mix was subsequently used to infect hACE2-293T cells (3×10^4 cells/ well) in the 96-well microplate (Corning, Cat#3917). After incubation for 48 h, an equal volume of One-Glo reagent (Promega, E6120) was added to the culture medium for readout. The percentage inhibition was calculated based on relative light units (RLUs) of the virus control and subsequently analyzed using a four-parameter logistic curve (GraphPad Prism 9.0).

FO-BLI biosensor detecting assay

The FO-BLI detection protocol is as previously described with some modification [35]. Shortly, Biotinylated hACE2-functionalized sensors were employed to capture SARS-CoV-2 NAbs via competitive binding. DAB, as a signal enhancer, and HRP-conjugated RBD (RBD-HRP) were utilized in the assay for signal amplification and detection, and competition, respectively. In order to achieve adequate binding for the NAbs biosensor, 5 μg/mL of biotinylated hACE2 in PBS-T buffer was utilized to induce loading shifts of approximately 1.0 nm. Prior to testing, RBD-HRP was combined in equal volumes with spiked samples. Between steps, washing was performed, and the signals produced were proportional to the quantity of RBD-HRP in the underlying complex. Specifically, SARS-CoV-2 (BA.4/BA.5/BA.5.2) Spike RBD Protein, SARS-CoV-2 XBB (Omicron) Spike RBD Protein and SARS-COV-2 BQ.1.1 (Omicron) Spike RBD Protein were ordered from SinoBiological (Beijing, China). All the mice sera were diluted 100-fold using a high-salt sample buffer, (i.e., PBS (10 mM, pH 7.4) containing 274 mM NaCl, 0.02% Tween20 and 0.1% BSA) to minimize the non-specific matrix interference. A mixed healthy mice serum collected from a mouse without vaccine administration was utilized as a control to calculate the relative inhibitory rate. The test was performed using Octet®

K2 2-Channel System, a RED96E 8-Channel System (Sartorius Group, Gottingen, Germany). Determination of neutralizing capacities by the FO-BLI biosensor was completed automatically within ten minutes.

Declaration of competing interest

The authors declare that they have no known competing financial interests or personal relationships that could have appeared to influence the work reported in this paper.

Author contribution

P.Q. and Z.C. supervised the study. Z.L. performed the experiment, collected data, analyzed data, wrote the first draft of the manuscript. S.B. detected NAbs with FO-BLI biosensor, analyzed data and revised the manuscript. S.Z. and X.Y. helped with the animal experiment. R.W., H.X. K.D., Y.C., P.W., and P.V. and R.W. helped revised the manuscript.

Acknowledgment

We thank the funding support from the Tsinghua Shenzhen International Graduate School Cross-disciplinary Research and Innovation Fund Research Plan, JC2022009; National Natural Science Foundation of China 31970752, 82104122; Science, Technology, Innovation Commission of Shenzhen Municipality JCYJ20190809180003689, JSGG20200225150707332, JCYJ20220530143014032, ZDSYS20200820165400003, WDZC20200820173710001, WDZC20200821150704001, JSGG20191129110812708; Shenzhen Bay Laboratory Open Funding, SZBL2020090501004; Department of Chemical Engineering-iBHE special cooperation joint fund project, DCE-iBHE-2022-3; and Bureau of Planning, Land and Resources of Shenzhen Municipality, (2022) 207.

Reference:

1. *Final efficacy, immunogenicity, and safety analyses of a nine-valent human papillomavirus vaccine in women aged 16–26 years: a randomised, double-blind trial.* The Lancet, 2017.
2. Dong, Y., et al., *A systematic review of SARS-CoV-2 vaccine candidates.* Signal Transduct Target Ther, 2020. **5**(1): p. 237.
3. Cao, Y., et al., *Omicron escapes the majority of existing SARS-CoV-2 neutralizing antibodies.* Nature, 2022. **602**(7898): p. 657-663.
4. Zhao, F., et al., *Challenges and developments in universal vaccine design against SARS-CoV-2 variants.* NPJ Vaccines, 2022. **7**(1): p. 167.
5. Qi, H., et al., *The humoral response and antibodies against SARS-CoV-2 infection.* Nat Immunol, 2022. **23**(7): p. 1008-1020.
6. Bao, L., et al., *The pathogenicity of SARS-CoV-2 in hACE2 transgenic mice.* Nature, 2020.

583(7818): p. 830-833.

7. Du, L., Y. Yang, and X. Zhang, *Neutralizing antibodies for the prevention and treatment of COVID-19.* Cell Mol Immunol, 2021. **18**(10): p. 2293-2306.
8. Kim, C., et al., *A therapeutic neutralizing antibody targeting receptor binding domain of SARS-CoV-2 spike protein.* Nat Commun, 2021. **12**(1): p. 288.
9. Pierri, C.L., *SARS-CoV-2 spike protein: flexibility as a new target for fighting infection.* Signal Transduct Target Ther, 2020. **5**(1): p. 254.
10. Kumar, S., K. Karuppanan, and G. Subramaniam, *Omicron (BA.1) and sub-variants (BA.1.1, BA.2, and BA.3) of SARS-CoV-2 spike infectivity and pathogenicity: A comparative sequence and structural-based computational assessment.* J Med Virol, 2022. **94**(10): p. 4780-4791.
11. Cao, Y., et al., *BA.2.12.1, BA.4 and BA.5 escape antibodies elicited by Omicron infection.* Nature, 2022. **608**(7923): p. 593-602.
12. Kurhade, C., et al., *Low neutralization of SARS-CoV-2 Omicron BA.2.75.2, BQ.1.1 and XBB.1 by parental mRNA vaccine or a BA.5 bivalent booster.* Nat Med, 2023. **29**(2): p. 344-347.
13. Scheaffer, S.M., et al., *Bivalent SARS-CoV-2 mRNA vaccines increase breadth of neutralization and protect against the BA.5 Omicron variant in mice.* Nat Med, 2023. **29**(1): p. 247-257.
14. Branche, A.R., et al., *Comparison of bivalent and monovalent SARS-CoV-2 variant vaccines: the phase 2 randomized open-label COVAIL trial.* Nat Med, 2023. **29**(9): p. 2334-2346.
15. Izikson, R., et al., *Safety and immunogenicity of a high-dose quadrivalent influenza vaccine administered concomitantly with a third dose of the mRNA-1273 SARS-CoV-2 vaccine in adults aged >/=65 years: a phase 2, randomised, open-label study.* Lancet Respir Med, 2022. **10**(4): p. 392-402.
16. Kang, Y.F., et al., *Quadrivalent mosaic HexaPro-bearing nanoparticle vaccine protects against infection of SARS-CoV-2 variants.* Nat Commun, 2022. **13**(1): p. 2674.
17. Liang, Q., et al., *RBD trimer mRNA vaccine elicits broad and protective immune responses against SARS-CoV-2 variants.* iScience, 2022. **25**(4): p. 104043.
18. Abbasi, J., *What to Know About EG.5, the Latest SARS-CoV-2 "Variant of Interest".* JAMA, 2023. **330**(10): p. 900-901.
19. Qu, P., et al., *Enhanced evasion of neutralizing antibody response by Omicron XBB.1.5, CH.1.1, and CA.3.1 variants.* Cell Rep, 2023. **42**(5): p. 112443.
20. Zhang, R., et al., *RCMNet: A deep learning model assists CAR-T therapy for leukemia.* Computers in Biology and Medicine, 2022. **150**: p. 106084.
21. Bhardwaj, V., et al., *Machine learning for endometrial cancer prediction and prognostication.* Frontiers in Oncology, 2022. **12**: p. 852746.
22. Liu, Y., et al., *Mixed-UNet: Refined class activation mapping for weakly-supervised semantic segmentation with multi-scale inference.* Frontiers in Computer Science, 2022. **4**: p. 1036934.
23. Hassan, M., et al., *Neuro-symbolic learning: Principles and applications in ophthalmology.* arXiv preprint arXiv:2208.00374, 2022.
24. Arevalo, C.P., et al., *A multivalent nucleoside-modified mRNA vaccine against all*

known influenza virus subtypes. Science, 2022. **378**(6622): p. 899-904.

25. Chaudhary, N., D. Weissman, and K.A. Whitehead, *mRNA vaccines for infectious diseases: principles, delivery and clinical translation.* Nat Rev Drug Discov, 2021. **20**(11): p. 817-838.
26. Pardi, N., et al., *mRNA vaccines - a new era in vaccinology.* Nat Rev Drug Discov, 2018. **17**(4): p. 261-279.
27. Ndeupen, S., et al., *The mRNA-LNP platform's lipid nanoparticle component used in preclinical vaccine studies is highly inflammatory.* iScience, 2021. **24**(12): p. 103479.
28. Fan, D., et al., *Self-shrinking soft demoulding for complex high-aspect-ratio microchannels.* Nature Communications, 2022. **13**(1): p. 5083.
29. Sarma, A.V., et al., *Solution NMR of a 463-residue phosphohexomutase: domain 4 mobility, substates, and phosphoryl transfer defect.* Biochemistry, 2012. **51**(3): p. 807-819.
30. Baden, L.R., et al., *Efficacy and Safety of the mRNA-1273 SARS-CoV-2 Vaccine.* N Engl J Med, 2021. **384**(5): p. 403-416.
31. Jackson, L.A., et al., *An mRNA Vaccine against SARS-CoV-2 - Preliminary Report.* N Engl J Med, 2020. **383**(20): p. 1920-1931.
32. Pegu, A., et al., *Durability of mRNA-1273 vaccine-induced antibodies against SARS-CoV-2 variants.* Science, 2021. **373**(6561): p. 1372-1377.
33. Hsieh, C.L., et al., *Structure-based design of prefusion-stabilized SARS-CoV-2 spikes.* Science, 2020. **369**(6510): p. 1501-1505.
34. Martinez-Flores, D., et al., *SARS-CoV-2 Vaccines Based on the Spike Glycoprotein and Implications of New Viral Variants.* Front Immunol, 2021. **12**: p. 701501.
35. Bian, S., M. Shang, and M. Sawan, *Rapid biosensing SARS-CoV-2 antibodies in vaccinated healthy donors.* Biosens Bioelectron, 2022. **204**: p. 114054.
36. Xia, X., *Detailed Dissection and Critical Evaluation of the Pfizer/BioNTech and Moderna mRNA Vaccines.* Vaccines (Basel), 2021. **9**(7).
37. Granados-Riveron, J.T. and G. Aquino-Jarquin, *Engineering of the current nucleoside-modified mRNA-LNP vaccines against SARS-CoV-2.* Biomed Pharmacother, 2021. **142**: p. 111953.
38. Beissert, T., et al., *A Trans-amplifying RNA Vaccine Strategy for Induction of Potent Protective Immunity.* Mol Ther, 2020. **28**(1): p. 119-128.
39. Chalkias, S., et al., *Three-month antibody persistence of a bivalent Omicron-containing booster vaccine against COVID-19.* Nat Commun, 2023. **14**(1): p. 5125.
40. Petrova, V.N. and C.A. Russell, *The evolution of seasonal influenza viruses.* Nat Rev Microbiol, 2018. **16**(1): p. 47-60.
41. Markov, P.V., et al., *The evolution of SARS-CoV-2.* Nat Rev Microbiol, 2023. **21**(6): p. 361-379.
42. Chen, Q., et al., *CRISPR–Cas12‐based field‐deployable system for rapid detection of synthetic DNA sequence of the monkeypox virus genome.* Journal of Medical Virology, 2023. **95**(1): p. e28385.
43. Bahri, M., et al., *Laser-Induced graphene electrodes for highly sensitive detection of DNA hybridization via consecutive cytosines (polyC)-DNA-based electrochemical*

biosensors. Microchemical Journal, 2023. **185**: p. 108208.